SECTION II. TASK 2. SUBMODEL DEVELOPMENT AND EVALUATION

Objectives

The objectives of this task are to develop or adapt advanced physics and chemistry submodels for the reactions of coal in an entrained-bed and a fixed-bed reactor and to validate the submodels by comparison with laboratory scale experiments.

Task Outline

The development of advanced submodels for the entrained-bed and fixed-bed reactor models will be organized into the following categories: a) Coal Chemistry (including coal pyrolysis chemistry, char formation, particle mass transfer, particle thermal properties, and particle physical behavior); b) Char Reaction Chemistry at high pressure; c) Secondary Reactions of Pyrolysis Products (including gas-phase cracking, soot formation, ignition, char burnout, sulfur capture, and tar/gas reactions); d) Ash Physics and Chemistry (including mineral characterization, evolution of volatile, molten and dry particle components, and ash fusion behavior); e) Large Coal Particle Effects (including secondary reactions within the particle and in multiple particle layers; f) Large Char Particle Effects (including oxidation); g) SO_x-NO_x Submodel Development (including the evolution and oxidation of sulfur and nitrogen species); and h) SO_x and NO_x Model Evaluation.

II.A. SUBTASK 2.a. - COAL TO CHAR CHEMISTRY SUBMODEL DEVELOPMENT AND EVALUATION

Senior Investigators - David G. Hamblen and Michael A. Serio
Advanced Fuel Research, Inc.
87 Church Street, East Hartford, CT 06108
(203) 528-9806

Objective

The objective of this subtask is to develop and evaluate, by comparison with laboratory experiments, an integrated and compatible submodel to describe the organic chemistry and physical changes occurring during the transformation from coal to char in coal conversion processes.

Accomplishments

During the past quarter, most of the effort was on using the set of rank dependent kinetic parameters obtained from low heating rate experiments to predict high heating rate data from pyrolysis experiments in our Transparent Wall Reactor (TWR) and Heated Tube Reactor (HTR). We also did simulations of high heating rate pyrolysis data from the literature such as the heated grid experiments of Gibbins, the wire grid experiments of Fong and coworkers of MIT, and the TWR experiments of Fletcher at Sandia.

Some problems were obtained in predicting the changes in the tar yield and tar molecular weight distributions with heating rate for low rank coals using the current version of the model. In addition, we could not predict the extractables yields for the high heating rate data of Fong and coworkers on the Pittsburgh Seam coal with the current kinetic parameters. It was decided to re-examine the assumptions on the model input parameters, such as 1) the bridge breaking rate, 2) the crosslinking efficiencies, 3) the tar vaporization law, and 4) the ΔP parameter. It was found that a modest change in the activation energy for the bridge breaking rate (from 25 to 27 kcal/mole) allowed for good predictions of the Fong data. Changes in the crosslinking efficiencies were thoroughly evaluated and found to be largely unnecessary. A decision was made

to use $10^{14}sec^{-1}$ for the bridge breaking pre-exponential and values of the crosslinking efficiencies = 1. The final set of rank dependent parameters is summarized in Table II.A-1.

The effects of the tar vaporization law and the ΔP parameter were found to be very important. The change in the original vaporization law from the expression proposed by Suuberg to a factor of 10 higher was found to be mainly responsible for the inability to predict the high heating rate Zap data. By changing to Suuberg X1, and allowing ΔP to be the sole adjustable parameter, the predictions are much better. A decision was initially made to use the law proposed by Fletcher, since it had been subjected to a rather thorough validation with model compounds. However, in the intermediate molecular weight range where the model is sensitive to the vaporization law, the two models are comparable. Therefore, either Fletcher or Suuberg X1 can be employed. The main unresolved question is the appropriate choice for ΔP and how this could be functionalized. It appears that the model predictions of the FIMS data are very sensitive to the choice of this parameter. At low heating rates, a choice of ΔP = 0 gives the best prediction of the tar yield. A choice of ΔP = 0.2 gives the best prediction of the tar MWD. Possible solutions would be to: 1) parameterize ΔP; 2) improve the description of the external transport of tar to resolve the problem of the higher molecular weight tars coming out earlier than expected.

Work continued on testing the fluidity model in conjunction with the changes in the FG-DVC model discussed above. For certain coals, such as Illinois No. 6 and Pocahontas, it is difficult to provide very good fits to both the fluidity and pyrolysis data. We also do not predict the fluid behavior of low rank coals which soften when heated to very high heating rates. However, we have achieved excellent agreement with the majority of data obtained sc far.

Work also continued on the swelling model. The changes in the FG-DVC model discussed above result in better predictions of the Free Swelling Index (FSI) for the majority of coals. There are still problems in fitting the FSI for the Pocahontas coal, which has a high FSI and a low Geissler fluidity.

TABLE II-A-1 - RANK DEPENDENT KINETIC PARAMETERS FOR ARGONNE PREMIUM COALS

KINETIC PARAMETERS		ZAP	WYO	ILL	UTAH	LS	PIT	UPF	POC
Bridge Breaking	A	1.0×10^{14}	1.0×10^{14}	1.0×10^{14}	1.0×10^{14}	1.0×10^{14}	1.0×10^{14}	1.0×10^{14}	1.0×10^{14}
	E/R	26,000	26,000	25,000	27,000	27,250	27,500	28,250	29,500
	σ/R	1,000	1,000	1,000	1,250	1,000	1,250	1,250	750
CH_4 Loose	A	3.0×10^{13}	3.0×10^{13}	3.0×10^{13}	3.0×10^{13}	3.0×10^{13}	3.0×10^{13}	3.0×10^{13}	3.0×10^{13}
	E/R	28,000	28,000	28,000	28,000	28,000	28,000	28,750	29,500
	σ/R	2,500	2,250	1,800	1,500	1,200	1,300	800	750
	wt.%	1.04	1.26	1.63	1.64	1.49	1.80	1.92	1.59
CH_4 Tight	A	6.0×10^{13}	6.0×10^{13}	6.0×10^{13}	6.0×10^{13}	6.0×10^{13}	6.0×10^{13}	6.0×10^{13}	6.0×10^{13}
	E/R	32,000	32,000	32,000	32,000	32,000	32,000	32,000	33,000
	σ/R	2,200	2,000	2,200	2,200	2,200	2,200	2,000	1,700
	wt.%	0.56	0.84	2.17	2.56	3.02	3.20	3.73	2.71
CO_2 X-Loose	A	5.0×10^{12}	5.0×10^{12}	5.0×10^{12}	5.0×10^{12}	5.0×10^{12}	5.0×10^{12}	5.0×10^{12}	5.0×10^{12}
	E/R	18,000	18,000	20,500	21,000	21,250	21,500	22,000	23,000
	σ/R	1,500	1,500	3,000	4,000	3,500	3,600	2,000	2,500
	wt.%	0.74	0.54	0.12	0.10	0.08	0.10	0.05	0.06
CO_2 Loose	A	5.0×10^{12}	5.0×10^{12}	5.0×10^{12}	5.0×10^{12}	5.0×10^{12}	5.0×10^{12}	5.0×10^{12}	5.0×10^{12}
	E/R	23,500	24,000	24,750	25,000	26,000	26,500	27,000	28,000
	σ/R	2,000	2,500	1,750	1,250	3,000	3,000	3,000	2,500
	wt.%	3.35	3.29	0.35	0.29	0.19	0.25	0.14	0.08
CO_2 Tight	A	7.5×10^{12}	7.5×10^{12}	7.5×10^{12}	7.5×10^{12}	7.5×10^{12}	7.5×10^{12}	7.5×10^{12}	7.5×10^{12}
	E/R	31,000	32,000	32,000	32,000	32,000	32,000	32,000	33,500
	σ/R	3,000	2,800	2,750	5,000	3,200	2,500	2,500	2,700
	wt.%	2.11	1.57	0.53	1.22	0.73	0.65	0.31	0.46
H_2O Loose	A	5.0×10^{12}	5.0×10^{12}	5.0×10^{12}	5.0×10^{12}	5.0×10^{12}	5.0×10^{12}	5.0×10^{12}	5.0×10^{12}
	E/R	16,000	16,000	25,000	25,000	25,500	25,000	27,500	28,000
	σ/R	1,500	1,500	1,000	1,250	1,250	1,250	1,250	1,250
	wt.%	0.64	0.47	1.46	3.11	2.63	2.30	1.60	0.51
H_2O Tight	A	2.0×10^{14}	2.0×10^{14}	2.0×10^{14}	2.0×10^{14}	2.0×10^{14}	2.0×10^{14}	2.0×10^{14}	2.0×10^{14}
	E/R	28,500	28,500	32,000	32,000	32,000	32,000	34,000	35,000
	σ/R	4,750	3,500	5,000	2,500	2,500	2,500	3,500	3,000
	wt.%	12.13	8.89	9.79	5.08	4.88	4.28	3.73	0.96
CO Loose	A	5.0×10^{12}	5.0×10^{12}	5.0×10^{12}	5.0×10^{12}	5.0×10^{12}	5.0×10^{12}	5.0×10^{12}	5.0×10^{12}
	E/R	24,500	24,750	25,000	25,000	25,500	26,000	28,000	29,000
	σ/R	3,000	2,500	1,000	1,250	1,100	1,250	750	1,250
	wt.%	1.80	1.70	0.30	0.40	0.20	0.25	0.20	0.15
CO Tight	A	5.0×10^{12}	5.0×10^{12}	5.0×10^{12}	5.0×10^{12}	5.0×10^{12}	5.0×10^{12}	5.0×10^{12}	5.0×10^{12}
	E/R	30,000	30,250	30,500	30,500	30,500	30,750	31,500	32,000
	σ/R	3,000	3,000	2,000	2,000	1,600	1,900	1,400	1,500
	wt.%	2.62	3.54	1.69	2.32	1.36	1.51	0.74	0.15
CO X-Tight	A	2.0×10^{14}	2.0×10^{14}	2.0×10^{14}	2.0×10^{14}	2.0×10^{14}	2.0×10^{14}	2.0×10^{14}	2.0×10^{14}
	E/R	39,000	39,750	40,000	40,000	40,000	40,000	40,000	40,000
	σ/R	2,500	2,500	3,000	2,500	3,000	2,800	2,250	3,200
	wt.%	5.25	5.00	3.20	2.80	3.00	2.30	1.37	1.90

Some work was done on incorporating the redistribution of functional groups into the FG-DVC model. The current assumption is that the breaking of two ethylene bridges creates two methyl groups. However, this leads to an overprediction of the amount of methyls, especially in the case of low rank coals.

The current state of the FG-DVC model was summarized in a paper titled "Can Coal Science be Predictive?" which is included as Appendix A. The paper was originally prepared by Peter Solomon for his keynote address at the 1990 Australian Coal Science Conference (delivered in 12/90). It was revised for his Storch Award lecture (to be delivered in 4/91) and that version is included in Appendix A.

Plans

Complete work on the fluidity model. Resume work on the swelling model and the optical properties model. Initiate work on studying the evolution of sulfur and nitrogen species. Complete work on definition of submodel for char reactivity.

II.B. SUBTASK 2.B. - FUNDAMENTAL HIGH-PRESSURE REACTION RATE DATA

Senior Investigators - Geoffrey J. Germane and Angus U. Blackham
Brigham Young University
Provo, Utah 84602
(801) 378-2355 and 6536

Student Research Assistants - Charles R. Monson, Gary Peterson,
David Wheeler, and James Rigby

Objective

The overall objective of this subtask is to measure and correlate reaction rate coefficients for pulverized-coal char particles as a function of char burnout in oxygen at high temperature and pressure.

Accomplishments

Three components of the subtask have been identified to accomplish the objectives outlined above: 1) develop the laminar-flow, high-pressure, controlled-profile (HPCP) reactor, 2) prepare char at high temperature and pressure, and 3) determine the kinetics of char-oxygen reactions at high pressure. The HPCP reactor, capable of functioning at 400 psi (27 atmospheres), has been constructed to perform the fundamental reaction rate measurements required for the study. Data from another char oxidation study (atmospheric pressure) conducted at Brigham Young University will also be used.

Work continued during the last quarter on development of the optical particle imaging system and the reactor collection system. In addition, progress was made in preparing coal samples with the proper size classification for the upcoming char preparation and reaction rate tests.

High Pressure Reactor Development and Characterization

Work during the reporting period focused mainly on automating the facility for the reactivity tests, and assembly of the optical instrument. Computer software was written to support the data acquisition and heater control hardware that was previously interfaced to the reactor instrumentation and heaters. This software was successfully used during the reporting period for devolatilization tests. The program allows the microcomputer to record and provide readout of reactor temperatures, pressure, and gas flow rates. Algorithms operate in real time to convert sensor signals into engineering units and display them on the monitor. These data along with information concerning heater controllers, reactor configuration, coal/char type and size, particle feedrate, and oxidizer concentration is written to a file every minute during a test to provide a detailed record.

The program also provides control of the reactor heaters. After the user inputs a desired zone temperature, the heater controller setting is determined by the microcomputer using temperature measurements from the heat zone and a proportional/integral control scheme. The microcomputer then sends the proper control signal to the controller through a 4 - 20 mA current loop. The four heat zones are controlled concurrently. In addition to maintaining the desired reactor temperature, the control algorithm checks for suspect thermocouple measurements, ensures that the heaters stay below their maximum allowable temperature and controls the rate of temperature change to prevent breakage of ceramics in the reactor because of thermal shock. The control system reduces temperature deviation during a test and improves repeatability of reactor conditions for duplicate tests. The ease of reactor operation is also increased.

It has become apparent during testing that the preheater capacity was too low to provide high secondary gas temperatures with the 5.1 cm ID reaction tube at conditions of high pressure and short residence time. Modifications are being made to the preheater to improve its capacity. The preheater heating element will be surrounded by a 12.7 cm ID alumina tube. The secondary gas will flow through a bed of alumina pieces that will fill the void between the alumina tube and the preheater insulation. The large

increase in available heat transfer area in the bed will significantly improve the capacity of the preheater. The situation will also be improved through the use of a smaller reaction tube. The required gas flow rate and preheater capacity will be reduced by 86% when using a 1.9 cm ID reaction tube. High temperature ceramic fixtures are being designed to properly locate the small reaction tube within the large tube.

Under separate funding, the gas mixing station is being assembled. The station will consist of the hardware necessary to meter and mix two gas flows. Nitrogen and air will be mixed during char oxidation experiments to provide the desired oxygen concentration for the primary and secondary gas flows. All components of the system have been received and assembly is in progress.

Optical Instrumentation - The optical instrument is patterned after a system developed at Sandia National Laboratories for *in situ* measurement of single particle temperature, velocity and diameter (Tichenor *et al.*, 1984). This system obtains temperature measurements by two-color pyrometry and particle velocity and diameter measurements through the use of an image-plane, coded-aperture technique. A description of the instrument and its operation was given in the 15th Quarterly Report. Implementation of the optical instrument to accurately determine particle temperature history during char oxidation experiments will improve the accuracy of the reaction rate parameter determination.

A great deal of work has been carried out in cooperation with a separate, independently-funded research group at the Brigham Young University Combustion Laboratory that is developing a particle imaging and temperature measuring instrument nearly identical to the one under development for this project. During the reporting period, most of this joint effort has centered on the photomultiplier tube (PMT) signal conditioning. In its original configuration the dynamic response of the PMT signal was too slow to allow particle size measurements. A number of amplifiers and configurations have been tried in an effort to improve the signal. Circuits that provide current-to-voltage conversion and preamplification of the PMT output have been developed that provide sufficient dynamic response and signal level. Work is ongoing to increase the signal-to-noise ratio through filtering, thereby

improving particle size measurements and extending the detection limit to smaller, lower temperature particles, which will be important for both char oxidation and coal devolatilization studies.

The final obstacle to be overcome with the optical system is proper operation of the laser trigger. A large fraction of the laser radiation scattered from a particle is lost as the light passes through the lenses, coded aperture, and especially the beamsplitter of the system. Sufficient light is not available at the laser detector to discriminate between a particle and noise. It appears that the laser beam will need to be focused from its 800 mm waist diameter to 100 mm diameter at the optical control volume in order to increase the intensity of scattered light. A prism may also be used to redirect the scattered light to the laser detector, bypassing the beamsplitter. Simple signal conditioning of the laser detector output will also be required.

Tar/Char/Gas Collection System - The modifications to the collection and separation system, involving a quenched and sintered stainless steel tube which extends from the entrance of the collection probe to the virtual impactor nozzle, were completed under independent funding. Coal devolatilization tests in the HPCP were successfully conducted by researchers from two separate independent projects, in which the collection system performed properly.

Char Preparation at High Temperature and High Pressure

During the reporting period, efforts continued to decrease the particle size range of the fractions of the selected coals and to produce sufficient coal in the desired size ranges for the char oxidation tests. Presently, Utah Blind Canyon bituminous coal, North Dakota lignite and Pittsburgh No. 8 bituminous coal have been sized and stored in sufficient quantities for the test program.

A sample of Utah bituminous coal was studied with a scanning electron microscope to assess the size distribution of the coal particles. The coal had been sieved to a range of 64-75 μm but there was some uncertainty whether

any fine particles (<10 μm) had adhered to the larger coal particles of the desired range. The scanning electron micrographs (SEM) in Figures II.B-1 and 2 show a range of particle size from about 60-80 μm. There are so few smaller particles that their possible effect on devolatilization and subsequent oxidation is considered to be insignificant. Also, there don't appear to be any fine particles attached to larger coal particles.

Kinetics of Char-Oxygen Reactions at High Pressure

While the literature review continues, no results in this area were obtained during the reporting period since the optical particle temperature and imaging system is not yet operable.

Plans

Modifications to the preheater will be made to increase heat transfer to the primary air and the gas mixing station will be completed and placed into service. Final alignment of the optical instrument will be completed and signal conditioning for the PMT outputs will be improved to provide stronger, noise free signals. Modifications will be made to the laser trigger to provide proper operation. The instrument will also be completely enclosed in a light-tight cover that will attach to the HPCP reactor. Since any stray light introduced into the optical system drastically increases noise, this will improve the instrument accuracy and allow operation of the system with the room lights on.

Work will continue to carefully size coal particles prior to char preparation and oxidation. An experimental plan for char oxidation will be finalized using a predictive reaction code to suggest test conditions. It is hoped that the optical system will be completed so that char preparation and oxidation for some of the test coals can be initiated under carefully controlled conditions in the HPCP reactor.

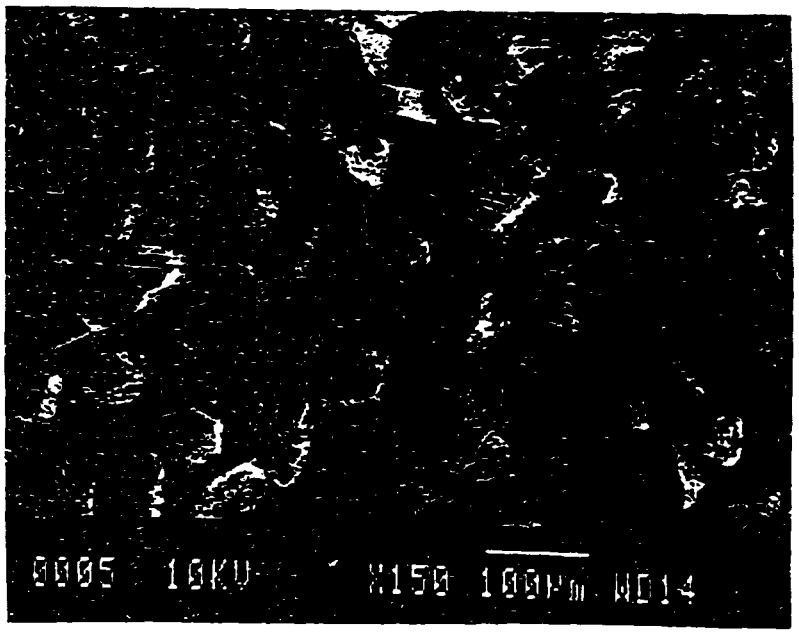

Figure II.B-1. Scanning electron micrograph of Utah Blind Canyon bituminous coal sieved to 64 - 75 μm.

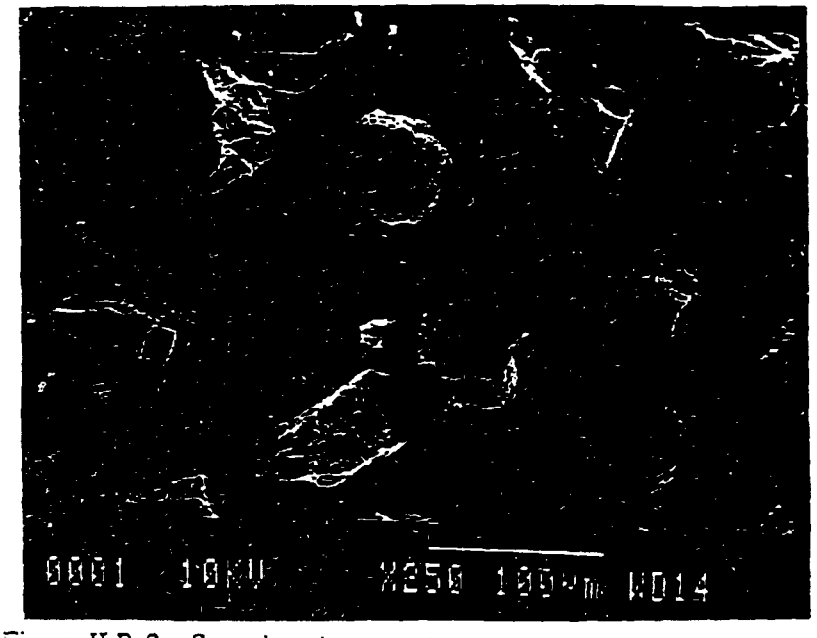

Figure II.B-2. Scanning electron micrograph of sieved 64 - 75 μm Utah Blind Canyon bituminous coal showing the extent of very small interspersed particles.

II.C. SUBTASK 2.c. - SECONDARY REACTION OF PYROLYSIS PRODUCTS AND CHAR BURNOUT

SUBMODEL DEVELOPMENT AND EVALUATION

Senior Investigator - James R. Markham and Michael A. Serio
Advanced Fuel Research, Inc.
87 Church Street, East Hartford, CT 06108
(203) 528-9806

Objective

The objective of this subtask is to develop and evaluate by comparison with laboratory experiments, an integrated and compatible submodel to describe the secondary reactions of volatile pyrolysis products and char burnout during coal conversion processes. Experiments on tar cracking, soot formation, tar/gas reactions, char burnout, and ignition will continue during Phase II to allow validation of submodels.

Accomplishments

Discussions were held with BYU on the future direction of the work on modeling the tomography data from the TWR coal flame experiments. Some discrepancies exist in the measured and predicted particle temperatures which could result from problems with the measurements and/or the model. A rate limiting step in comparing the model with the data is the generation of suitable plots. A new approach which involves output of the predictions of the model into a spreadsheet format was agreed upon.

Plans

Continue work with BYU on modeling the TWR coal flame experiments. Define submodels for ignition and soot formation.

II.D. SUBTASK 2.d. - ASH PHYSICS AND CHEMISTRY SUBMODEL

Senior Investigator - James Markham
Advanced Fuel Research, Inc.
87 Church Street, East Hartford, CT 06108
(203) 528-9806

Objective

The objective of this task is to develop and validate, by comparison with laboratory experiments, an integrated and compatible submodel to describe the ash physics and chemistry during coal conversion processes. AFR will provide the submodel to BYU together with assistance for its implementation into the BYU PCGC-2 comprehensive code.

To accomplish the overall objective, the following specific objectives are: 1) to develop an understanding of the mineral matter phase transformations during ashing and slagging in coal conversion; 2) To investigate the catalytic effect of mineral matter on coal conversion processes. Data acquisition will be focused on: 1) design and implementation of an ash sample collection system; 2) developing methods for mineral characterization in ash particles; 3) developing methods for studying the catalytic effects of minerals on coal gasification.

Accomplishments

No work scheduled during the past quarter.

Plans

Complete definition of submodel for ash chemistry and physics.

II.E. SUBTASK 2.e. - LARGE PARTICLE/THICK BED SUBMODELS

Senior Investigator - Michael A. Serio
Advanced Fuel Research, Inc.
87 Church Street
East Hartford, CT 06108
(203) 528-9806

Objective

The objectives of this task are to develop or adapt advanced physics and chemistry submodels for the reactions of "large" coal particles (i.e., particles with significant heat and/or mass transport limitations) as well as thick beds (multiple particle layers) and to validate the submodels by comparison with laboratory scale experiments. The result will be coal chemistry and physics submodels which can be integrated into the fixed-bed (or moving-bed) gasifier code to be developed by BYU in Subtask 3.b. Consequently, this task will be closely coordinated with Subtask 3.b.

Accomplishments

The work on the modified AFR fixed-bed reactor (FBR) system continued. It includes two independently heated stages. The reactor system was assembled and tested and is now being used for lignin pyrolysis experiments under independent funding. It appears to work as planned. A redesign of the upper reactor chamber was required in order to eliminate a tar deposition problem. As expected, the quantitation of gas and tar is much better than in the old system and a wider range of sample sizes and flow rates can be used. Some problems were encountered with the software used to quantify the IR data, but these appear to have been resolved.

Plans

Complete testing of new fixed-bed reactor system. Complete initial set of experiments on secondary reaction effects in thick beds. Continue development of single particle model with BYU. Begin work on tar repolymerization model.

II.F. SUBTASK 2.F. - LARGE PARTICLE OXIDATION AT HIGH PRESSURES

Senior Investigators: Angus U. Blackham and Geoffrey J. Germane
Brigham Young University
Provo, Utah 84602
(801) 378-2355 and 6536

Student Research Assistants: Ken Bateman, Gary Pehrson and Wade Riser

Objectives

The overall objective for this subtask is to provide data for the reaction rates of large char particles of interest to fixed-bed coal gasification systems operating at pressure. The specific objectives for this quarter included:

1. Review appropriate literature.
2. Select the experimental approach.
3. Design the apparatus to use in conjunction with the HPCP reactor of Subtask 2b.
4. Request support information concerning the proposed "cantilever beam insert."
5. Continue evaluation of analytical procedures for monitoring the kinetics of oxidation of large particles.
6. Conduct additional preliminary oxidation experiments.

Accomplishments

Two components of this subtask to accomplish the overall objective have been suggested in the plans outlined earlier: 1) high-pressure, large-particle reactor design, fabrication and preliminary data: 2) experimental reaction rate data for chars from five coals. The general features of the experimental unit will be a "large particle insert" to be connected to the HPCP facility of Subtask 2b. The "large particle insert" will consist of: (a) the reactor tube, (b) the balance unit, and (c) the connecting channel. Of the two experimental approaches considered in previous reports, the decision has been made to develop the "cantilever beam insert." In this

approach, the sample will be mounted horizontally from a force transducer connected to one or two of the optical access ports of the HPCP reactor.

In this quarter, a summary of the design of the "cantilever beam insert" was prepared and sent to a few principal investigators active in fields of closely related research for their comments and criticisms. Some responses have been received and evaluated. These suggestions have expanded the basis on which the design details of the cantilever beam insert are now progressing.

A few additional experimental exercises with the load cell have given additional information on the properties of the load cell. Because of a change in personnel on this subtask the evaluation of the CO/CO_2 chromatographic column has not yet been completed. The report of this evaluation will be included in the next quarterly report. The air oxidation of sets of large coal particles in platinum crucibles is continuing. The variables in these preliminary studies are coal type, size and temperature. These results will be compared with the results of the preliminary oxidation of the Utah bituminous coal reported previously in the 4th Annual Report (Solomon, 1990).

High-Pressure, Large-Particle Reactor Design

Experimental Approach - Reactor Design - After the decision was made to develop the "cantilever beam insert," a summary of the features of this proposed experimental facility was prepared and given to a few principal investigators active in fields of research closely related to our project of large coal particle oxidation with a request for their suggestions concerning the design features. This five page "Request for Informal Design Review" is included in the appendix of this quarterly report. The responses received have been reviewed and evaluated. Some design features have been added or modified as a result of these responses. The general design, however, has remained unchanged, and the detailed drawings for the "cantilever beam insert" are being prepared. Construction of the facility will start in this next quarter.

Experimental Approach - Force Transducer - During this quarter, a few additional tests were made with the load cell (force transducer) to determine its properties. Measurements of maximum load, stability, and sensitivity were made as a function of lever-arm length. Lever-arms of 10, 15 and 20 cm were studied. The maximum loads measured were 25, 22 and 19 g, respectively. The drift of the transducer was a maximum at 10 mg/hr showing good stability at maximum loads. The sensitivity is still ~3 mg per division at each length. Improving this sensitivity to 1 mg per division in still considered possible as further testing and adjusting of the amplifier-indicator is accomplished.

Experimental Reaction Rate Data

Preliminary Large Particle Oxidation Measurements - For the principal purpose of providing experience in experimental procedures associated with large coal particles, a series of sets of large particles of a Utah bituminous coal have been devolatilized and oxidized in platinum crucibles. A lump of coal was crushed to provide some particles with dimensions about 0.5-1.0 cm on a side. The first set (six particles) was heated with Mekker burners. The results were given in the 14th Quarterly Report (Solomon et al., 1990). A second set (six particles) was heated in a muffle furnace and reported in the 15th Quarterly Report (Solomon, 1990). Four sets of samples (four particles in each set) were heated at different temperatures in the muffle furnace. The results were reported in the 4th Annual Report (Solomon et al., 1990).

An additional study of the data of these last four sets has been made, resulting in a correlation not noted in the earlier reports. Graphs of each of the four sets of data have been prepared with the log of the normalized mass remaining for each particle plotted against the time of oxidation. The slope of each curve therefore is an indication of mass reactivity. The average mass reactivities for the sixteen particles reported in Table II.F - 2 of the 4th Annual Report are included in Figures II.F-1, 2, 3, and 4 along with the initial mass of each large particle. Our expectation was that average mass reactivity would correlate with temperature of oxidation. There was a slight indication of this because the highest observed mass reactivity was at the highest oxidation temperature (0.112 min^{-1} at 1420-1470 K). However the spread of reactivities of the four particles in this temperature

Experimental Approach - Force Transducer - During this quarter, a few additional tests were made with the load cell (force transducer) to determine its properties. Measurements of maximum load, stability, and sensitivity were made as a function of lever-arm length. Lever-arms of 10, 15 and 20 cm were studied. The maximum loads measured were 25, 22 and 19 g. respectively. The drift of the transducer was a maximum at 10 mg/hr showing good stability at maximum loads. The sensitivity is still ~3 mg per division at each length. Improving this sensitivity to 1 mg per division in still considered possible as further testing and adjusting of the amplifier-indicator is accomplished.

Experimental Reaction Rate Data

Preliminary Large Particle Oxidation Measurements - For the principal purpose of providing experience in experimental procedures associated with large coal particles, a series of sets of large particles of a Utah bituminous coal have been devolatilized and oxidized in platinum crucibles. A lump of coal was crushed to provide some particles with dimensions about 0.5-1.0 cm on a side. The first set (six particles) was heated with Mekker burners. The results were given in the 14th Quarterly Report (Solomon et al., 1990). A second set (six particles) was heated in a muffle furnace and reported in the 15th Quarterly Report (Solomon, 1990). Four sets of samples (four particles in each set) were heated at different temperatures in the muffle furnace. The results were reported in the 4th Annual Report (Solomon et al., 1990).

An additional study of the data of these last four sets has been made, resulting in a correlation not noted in the earlier reports. Graphs of each of the four sets of data have been prepared with the log of the normalized mass remaining for each particle plotted against the time of oxidation. The slope of each curve therefore is an indication of mass reactivity. The average mass reactivities for the sixteen particles reported in Table II.F - 2 of the 4th Annual Report are included in Figures II.F-1, 2, 3, and 4 along with the initial mass of each large particle. Our expectation was that average mass reactivity would correlate with temperature of oxidation. There was a slight indication of this because the highest observed mass reactivity was at the highest oxidation temperature (0.112 min-1 at 1420-1470 K). However the spread of reactivities

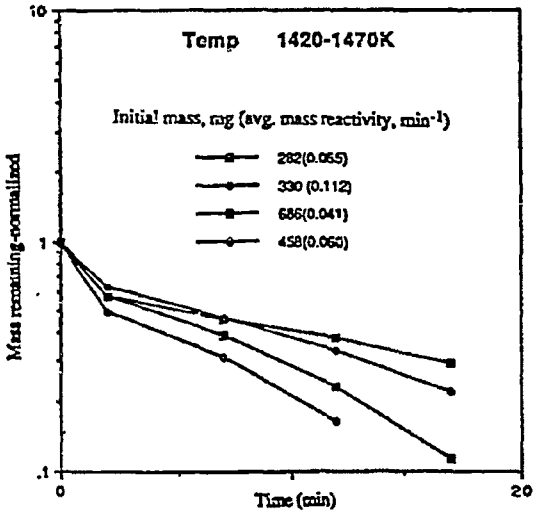

Figure II.F-1. Mass of large coal particles remaining (normalized) as a function of reaction time at 1420 - 1470 K.

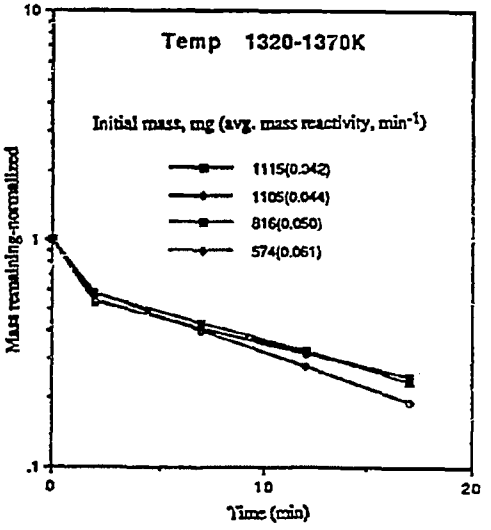

Figure II. F-3. Mass remaining (normalized as a function of reaction time at 1320 - 1370 K.

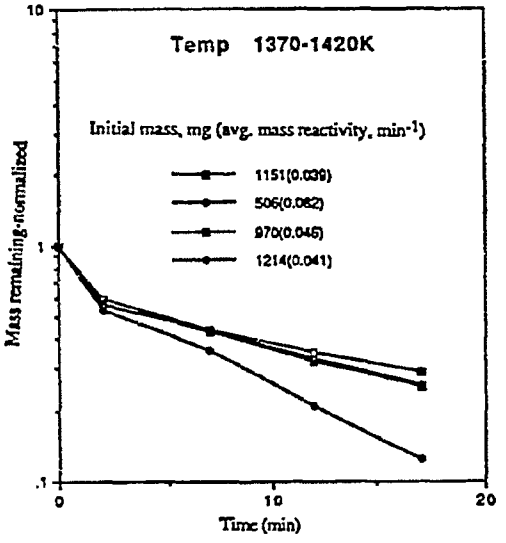

Figure II.F-2. Mass remaining (normalized) as a function of reaction time at 1370 - 1420 K.

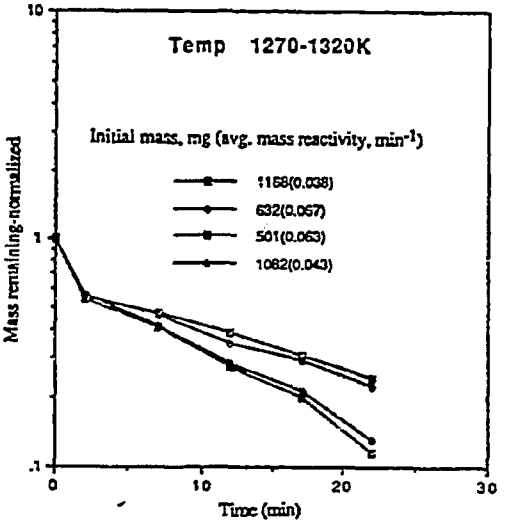

Figure II. F-4. Mass remaining (normalized) as a function of reaction time at 1270 - 1320 K.

range was quite broad (0.041 to 0.112 min^{-1}) and appeared to be a function of the initial particle mass. When the average mass reactivity for all sixteen particles was plotted against initial particle mass, the correlation presented in Figure II.F-5 was obtained. All four temperature ranges are represented in the cluster of points for initial masses greater than 1 gram. Therefore, in the overall temperature range for these oxidations, mass reactivity does not appear to change significantly with temperature but decreases with increasing particle mass. This observation suggests that the factor of most influence under these conditions is the movement of gas through the developing ash residue for this range of temperatures (1270-1470K).

This preliminary conclusion, along with those suggested in the previous reports, indicates that further experiments of this preliminary nature with platinum curcibles at atmospheric pressure will help in determining the issues that need to be considered as plans are being made for measurements at high pressure in the facility to be constructed for this subtask. Accordingly, experiments are currently in progress in which the variables are coal type, size and temperature.

Plans

During the next quarter, construction of the "cantilever beam insert" will start. The study of the load cell will continue as it is incorporated into the balance unit. Evaluation of the CO/CO_2 gas chromatographic column will be completed. Additional preliminary experiments will be completed and compared with those discussed here and in previous reports.

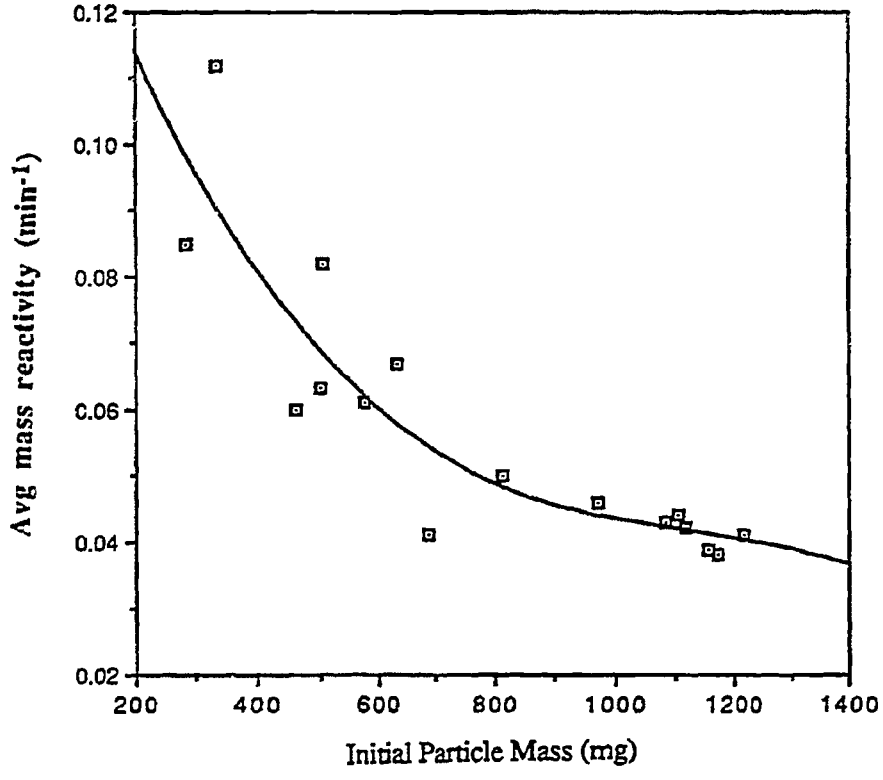

Figure II. F-5. Effect of initial particle mass on average mass reactivity for various temperatures from 1270 - 1470 K.

II.G. SUBTASK 2.G. - SO_x/NO_x SUBMODEL DEVELOPMENT

Senior Investigators: L. Douglas Smoot and B. Scott Brewster
Brigham Young University
Provo, Utah 84602
(801) 378-4326 and (801) 378-6240

Research Assistant: Richard D. Boardman

Objectives

The objectives of this subtask are 1) to extend an existing pollutant submodel in PCGC-2 for predicting NO_x formation and destruction to include thermal NO, 2) to extend the submodel to include SO_x reactions and SO_x-sorbent reactions (effects of SO_3 nonequilibrium in the gas phase will be considered), and 3) to consider the effects of fuel-rich conditions and high-pressure on sulfur and nitrogen chemistry in pulverized-fuel systems.

Accomplishments

The task of extending the NO_x submodel to include thermal NO has been completed. The fuel-NO mechanism was also generalized to test alternative global rate expressions, including NH_3 as an intermediate species. An evaluation of the NO_x submodel was completed and reported in the 4th Annual Report (Solomon et al., 1990). During the past quarter, the method used to determine atomic oxygen concentrations was revisited. Further insight into the best quasi-equilibrium expression to use for predicting atomic oxygen concentrations in lean, swirling-flow, natural gas flames was gained.

Work has continued on the development and evaluation of a SO_x/sorbent reaction computerized submodel. The framework for this submodel was presented and briefly discussed in the 4th Annual Report (Solomon et al., 1990). This code has been integrated into PCGC-2 and is currently being evaluated. Several simplifications are made in this "first-generation" model which may

not be valid for all reactor conditions. The complexity of the model can be increased after demonstration of a suitable sulfur capture model.

In the current quarterly report, the theory of the SO_x submodel is further discussed. A preliminary prediction that was completed is discussed. Work is continuing to verify that the model predicts correct results, prior to a more extensive evaluation of the model.

NO_x Submodel Development

Investigation of the expression used to estimate atomic oxygen concentrations was further explored using the NO formation rate expression derived from the Zel'dovich thermal-NO mechanism (Westenberg, 1971):

$$\frac{d[NO]}{dt} = 2k_{A6}[O][N_2] \quad \text{gmole cm}^{-3}\,\text{s}^{-1} \qquad \text{(II.G-1)}$$

This expression is obtained by assuming the reverse Zel'dovich mechanism steps are negligible and that OH concentrations are small.

Two quasi-equilibrium expressions are often used to estimate O concentrations. Oxygen equilibrium (Eq. II.G-2) has been recommended for fuel-lean zones in the combustor while carbon equilibrium (Eq. II.G-3) has been suggested for fuel-rich regions where primary fuel oxidation occurs.

$$[O] = \left\{K_{eq}^{\cdot}[O_2]\right\}^{1/2} \qquad \text{(II.G-2)}$$

$$[O] = K_{eq}^{\cdot}\frac{[O_2][CO]}{[CO_2]} \qquad \text{(II.G-3)}$$

The sensitivity of the NO model to these expressions was examined to determine if either or both expressions should be used to predict atomic oxygen concentrations. Figure II.G-1 compares the predicted NO concentrations with the experimental values measured in the ACERC controlled-profile reactor (with independent funding) over a narrow range of overall fuel-to-oxidizer equivalence ratios with an experimental secondary-air swirl number of 1.5. Separate NO model predictions were made using either oxygen equilibrium or carbon equilibrium at every computational node in the reactor to predict

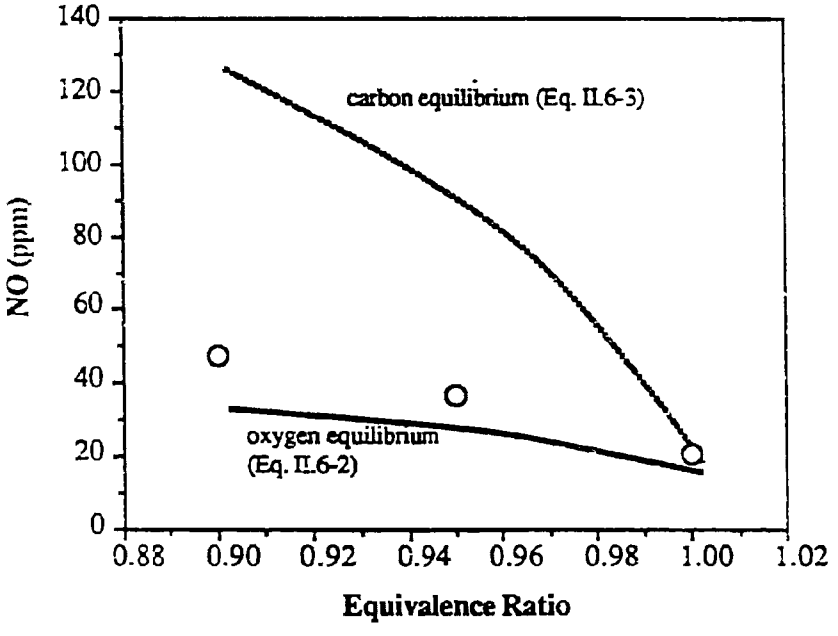

Figure II. G-1. Comparison of prediction methods used to estimate atomic oxygen concentrations with measured data (circles) for natural gas combustion in the ACERC controlled-profile reactor. Secondary swirl no. - 1.5; heating rate = 147 kW.

atomic oxygen concentrations. The upper theoretical curve shows that thermal NO concentrations are overpredicted at lower equivalence ratios (fuel-lean conditions) when carbon equilibrium is assumed. When oxygen equilibrium is assumed, predicted NO concentrations are lower than the measured data. Predictions were not made for higher equivalence ratios for which the importance of carbon equilibrium may lead to better prediction of atomic oxygen concentrations. The results in this study are thus limited, but hopefully provide guidance for using the NO model for practical burner conditions, which are normally fuel-lean to achieve complete combustion.

SO_x-Sorbent Particle Reaction Submodel

Submodel Description - Implementation of a SO_x/sorbent-reactions submodel into PCGC-2 is broken down into three components: 1) describing the simultaneous conversion of coal sulfur to gaseous species, 2) tracking the injected sorbents while accounting for simultaneous calcination, sintering, and sulfation, and 3) predicting simultaneous capture of sulfur species (usually H_2S and SO_2) by the sorbent particles. The approach taken to develop a SO_x/sorbent-reactions predictive model is to simplify the description of these three components as much as possible in order to first demonstrate the feasibility of predicting sorbent capture with a submodel of PCGC-2. Then, after an evaluation of the "first-generation" model is completed, assumptions can be relaxed as warranted by the verification procedure and other experimental evidence.

In the 4th Annual Report (Solomon et al., 1990), a brief discussion of the SO_x/sorbent-reactions submodel foundation was given. Figure II.G-2 illustrates the solution algorithm for the SO_x/sorbent-reactions submodel which is called after converging PCGC-2. As individual particle trajectories are integrated, the capture of SO_2 and H_2S is calculated at each time step by the shrinking-core grain model of Silcox (1985). Figure II.G-3 shows the individual steps contained in the sulfation submodel using the set of equations listed in Table II-G-1.

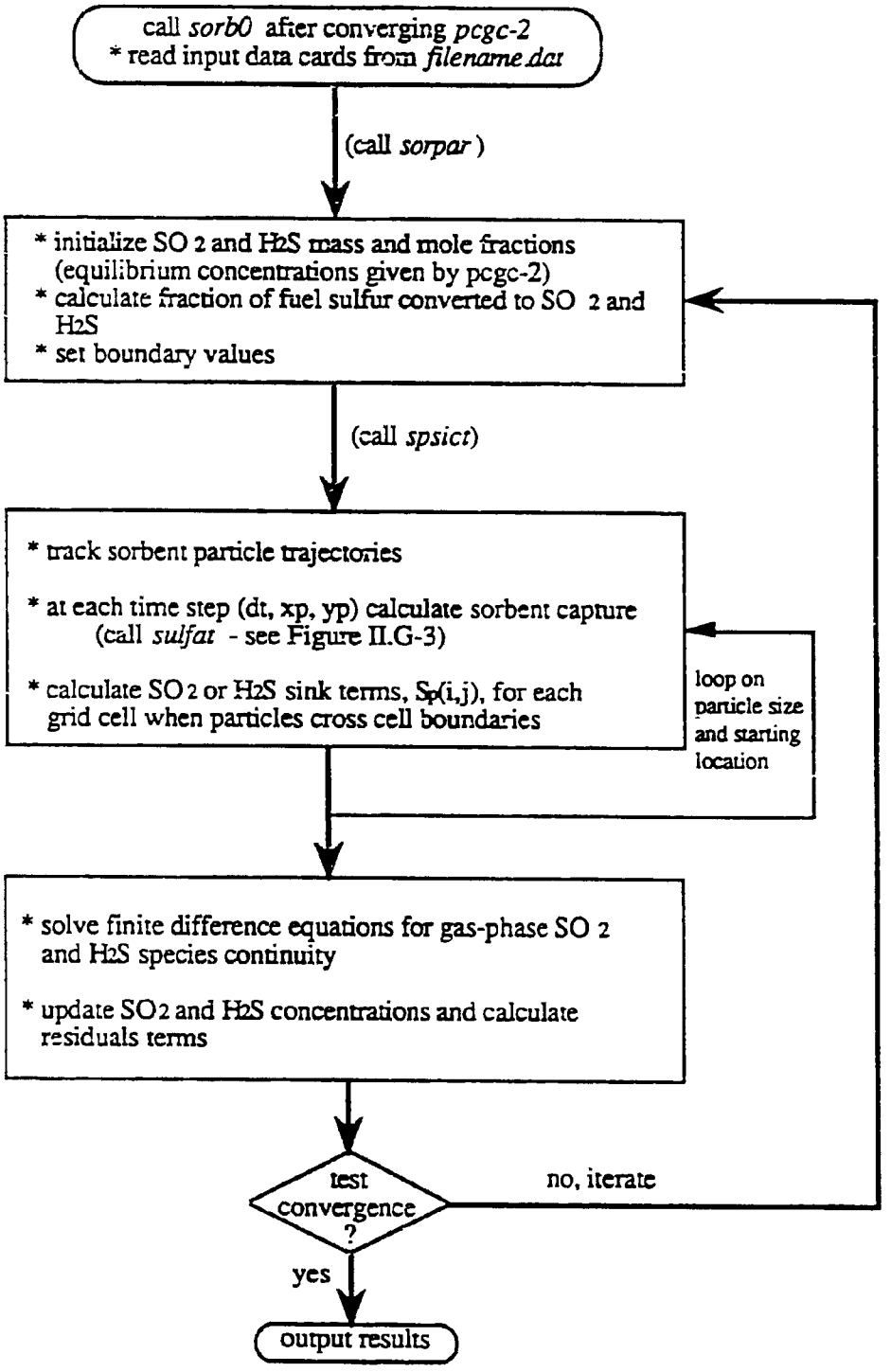

Figure II.G-2. SOx/sorbent reaction submodel solution algorithm.

sulfat (calculation of sorbent sulfation)
Called from spsict at time step along particle trajectory path

initialization
* select number of subshells to descibe sorbent particles
* calculate the radius of grains based on BET surface area of sorbent particles
* at each particle starting location, set initial conversion of grains to 1E-10 to avoid division by zero at first time step
  Also, set radius of unreacted CaO to (1.0-1E-10)*(initial grain radius) for each subshell and assign the concentration profiles of SO_2 and H_2S through the particles
* select order of sulfation reaction

at each time step (xp,yp, dt)
* calculate gas temperature, [SO_2], and [H_2S] by 2-D interpolation
* set the concentration of SO_2 and H_2S at the sorbent particles surface (node n) equal to [SO_2], and [H_2S]
* calculate the interfacial area available for reaction at each subshell
* calculate the particle void fraction as a function of sorbent particle radius
* calculate the extended grain radius (due to increase in the molar volume of $CaSO_4$ product) at each subshell
* calculate bulk and Knudsen diffusivity at each subshell
* calculate the effective diffusivity at each subshell
* calculate product layer diffusivity at each subshell
* calculate the reaction rate constant (assumed to be constant throughout the sorbent particle since particles are isothermal)

calculate new concentration profiles through the sorbent particle using material balance differential equation

first-order reaction
* assemble coefficients for matix solution
* use Thomas algorithm to solve tri-diagonal system of equation

half-order reaction
* assemble coefficients for matrix solution
* use Newton-Raphson technique to calculate concentration at each sorbent particle subshell

determine sorbent particle conversion due to reaction occurring during dt (differential time step)
* calculate change in grain radius due to reaction
* calculate conversion for each subshell
* obtain overall conversion for sorbent particle by summing up subshell
  conversion (integration procedure used)

return to *spsict*

Figure II.G-3. Sulfation model procedure outline. (See Table II.G-1 for equations).

Figure II.G-4 ***Predicted Sorbent SO_2 Capture***
Wyo. subbit. coal, 1:10 sorbent/coal feed

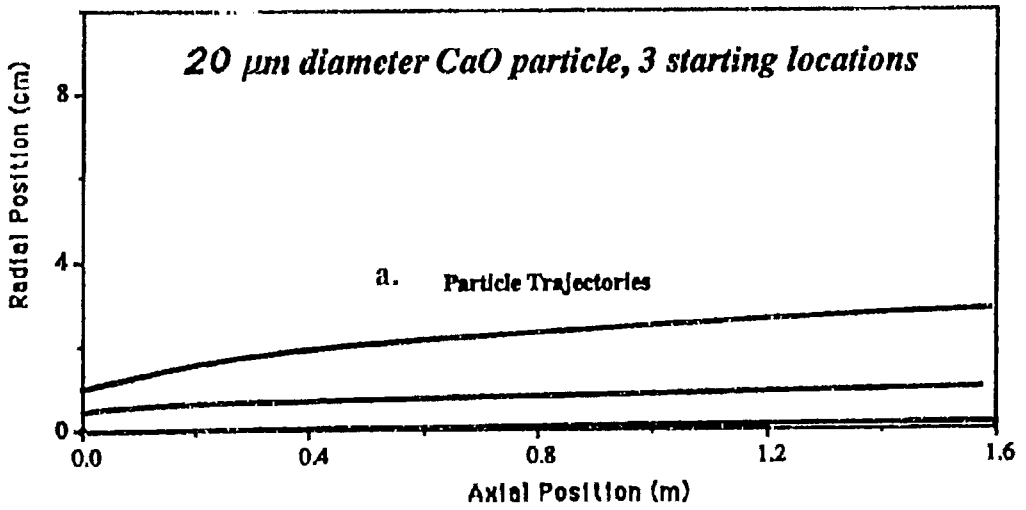

b. SO_2 *Concentration: without sorbent injection ———; with sorbent injection ———*

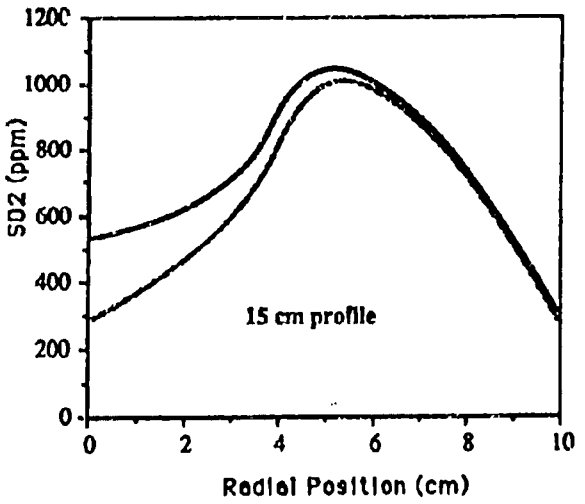

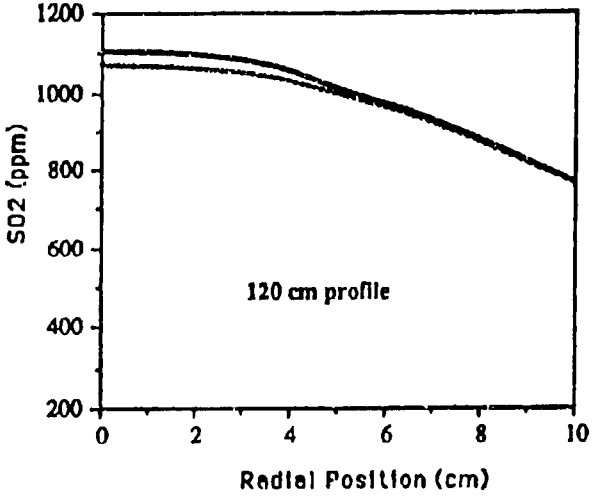

Table II.G-1. Sorbent-Reaction Submodel Equation Set

Equation	Definition	Eq. No.[5]
$\frac{d^2[SO_2]}{dR^2}+\left(\frac{2}{R}+\frac{1}{D_{eff}}\frac{dD_{eff}}{dR}\right)\frac{d[SO_2]}{dR}-\frac{N}{D_{eff}}=0.$	Material balance on SO_2 in a spherical shell Used to calculate [SO_2] at each sorbent particle subshell.	4.7
$@R=0.;\ \frac{d[SO_2]}{dR}=0.$ $@R=R_p;\ [SO_2]_{R_p}=[SO_2]_{xp,yp,zp}$	Boundary conditions	4.9
$N=k_{\frac{1}{2}}A[SO_2]^{\frac{1}{2}}_{r_{cor(i)}}$	Half-order volumetric consumption rate	4.10
$N=k_1A[SO_2]^{1}_{r_{cor(i)}}$	First-order volumetric consumption rate	4.11
$A=3z(1-e_c)\frac{r^3}{r^3_{cor(i)}}$	Interfacial area available for reaction at ith subsheli	4.15
$z=\left\{\frac{\rho_{CaO}}{\rho_{MgO}}\left(\frac{1}{W}-1\right)+1\right\}^{-1}$	Fraction of grains which are CaO	4.16
$W=\left\{1+\left(\frac{1-Y}{Y}\right)\left(\frac{M_{MgO}M_{CaCO_3}}{M_{MgCO_3}M_{CaO}}\right)\right\}^{-1}$	Weight fraction of CaO in the calcine on an "impurity-free" basis	4.17
$\frac{dr_{cor(i)}}{dt}=\left(\frac{-M_{CaO}}{\rho_{CaO}}\right)K_n[SO_2]^n_{r_{cor(i)}}$	Material balance on CaO at product-CaO interface for nth order reaction	4.13 4.14
$[SO_2]_{r_{cor(i)}}=\frac{D_{sp}[SO_2]_{R_{(i)}}}{D_{sp}+K_1r_{cor(i)}\left(1-\frac{r_{cor(i)}}{r_{ext(i)}}\right)}$	Interfacial concentration for ith subshell for first-order reaction rate	4.23
$[SO_2]_{r_{cor(i)}}=\frac{2[SO_2]_{R_{(i)}}-\alpha-\left(-4[SO_2]_{R_{(i)}}\alpha+\alpha^2\right)^{\frac{1}{2}}}{2}$ where, $\alpha=-\left(\frac{K_{\frac{1}{2}}r_{cor(i)}}{D_{sp}}\right)^2\left(1-\frac{r_{cor(i)}}{r_{ext(i)}}\right)^2$	Interfacial concentration for ith subshell for half-order reaction rate	4.24
$r_{ext(i)}=\left\{\left(\frac{r_g^3-r_{cor(i)}}{1-e_s}\right)\left(\frac{\rho_{CaO}M_{CaSO_4}}{\rho_{CaSO_4}M_{CaO}}\right)+r^3_{cor(i)}\right\}^{\frac{1}{3}}$	Extended grain radius	4.26

Table II.G-1 Continued

Equation	Definition	Eq. No.§
$r_g = \frac{3}{\rho_{CaO}(BET\ surface\ area)}$	Initial grain radius	4.84
$e_x = 1-(1-e_c)\left\{1+\left[\frac{\left(\frac{a}{1-e_s}-1\right)X}{1+\frac{\rho_{CaO}(1-W)}{\rho_{MgO}W}}\right]\right\}$	Particle void fraction	4.28
$X_{R(i)} = 1-\left(\frac{r_{cor(i)}}{r_g}\right)^3$	Extent of grain conversion at ith subshell	4.27
$X(t) = \frac{3}{R_p^3}\int_0^{R_p} R_{(i)}^2 X_{R(i)} dR$	Overall conversion of sorbent particle	4.44
$K_1 = 291\exp\left(\frac{-7510}{T}\right)$ $cm\,sec^{-1}$	First-order reaction rate constant	4.79a
$K_{1/2} = 0.0307\exp\left(\frac{-6970}{T}\right)$ $gmol^{\frac{1}{2}}cm^{-\frac{1}{2}}sec^{-1}$	Half-order reaction rate constant	4.79b
$D_{eff} = \left(\frac{1}{\frac{1}{D_M}+\frac{1}{D_K}}\right)e_x^2$	Effective diffusivity	4.80
$D_M = \exp(1.66\ln(T)-11.3)$ cm^2sec^{-1}	Bulk diffusivity for SO_2-air binary-pair	-
$D_K = 19{,}400\frac{e_c}{\rho_{CaO}(\text{BET surface area})}\sqrt{\frac{T}{M_{SO_2}}}$ cm^2sec^{-1}	Knudsen diffusion coefficient	4.82
$D_S = 0.0124\exp\left(\frac{-12{,}200}{T}\right)$ cm^2sec^{-1}	Product layer diffusion coefficient	4.83

§ Equations reference number in Silcox (1985). Rate constants and diffusion coefficients derived by Silcox from experimental data as cited by Silcox (1985)

As individual particles pass through computational cells in the reactor domain, the extent of sorbent conversion by the reactions:

$$CaO + SO_2 + 1/2O_2 \text{ --> } CaSO_4 \qquad \text{(II.G-4)}$$

$$CaO + H_2S \text{ --> } CaS + H_2O \qquad \text{(II.G-5)}$$

is predicted. Thus, the submodel predicts the loss (or sink) of gaseous sulfur species occurring in each computational cell. Species continuity is then solved for H_2S and/or SO_2 to determine the steady-state concentrations throughout the reactor. The complete source term for each cell also includes the release of sulfur species from the coal, given by the sulfur-species equilibrium ratio predicted by PCGC-2. As sulfur is captured by the sorbents, the gaseous sulfur species are assumed to re-equilibrate to the equilibrium ratio that is predicted without sulfur capture. These assumptions make it possible to decouple the SO_x/sorbent-reactions submodel from the main code.

The algorithm is iterative since the sulfation submodel is dependent on the concentrations of SO_2 and H_2S in the gas. Convergence is determined by summing up residual terms for species continuity and comparing these values with a small tolerance. This is a rigorous approach and ensures convergence of the differential equations for all regions of the reactor.

Key Submodel Assumptions - In the current SO_x/sorbent-reactions submodel the following assumptions are made with respect to the individual three components:

(.) Prediction of Gaseous SO_x Species Formation:

- Both inorganic and organic sulfur are released from coal at a rate proportional to total coal mass loss.
- Gaseous sulfur is instantaneously converted to an equilibrium composition of SO_2, SO_3, H_2S, COS, CS_2, etc. as soon as the sulfur is released from the coal and mixed locally with the bulk gas.
- As sulfur is captured by injected sorbents, the pool of sulfur species is proportionally reduced.
- Species continuity is solved to determine the steady-state concentration of sulfur species accounting for simultaneous sulfur release by coal and capture by sorbents.

(2) Sorbent Particle Calcination and Dispersion:

- Variable particle sizes are allowed.
- Particles are injected with the coal feed inlets (generalized inlet injections will be implemented later).
- Particles are rapidly calcined by the high temperatures encountered near the coal injection regions.
- Calcination gas (CO_2 if $CaCO_3$ sorbents or H_2O if $Ca(OH)_2$ sorbents) is added to the inlet carrier gas.
- Particles are in thermal equilibrium with the adjacent gas temperature.
- Particles are isothermal.
- Particles follow gas streamlines, accounting for turbulent dispersion effects.
- Energy and momentum coupling between sorbents and the gas are neglected (i.e., radiation absorption and attenuation are ignored).

(3) Sulfation of Sorbents (SO_2 Capture):

- Sorbent particles are comprised of tiny spherical grains of CaO, determined from BET surface area.
- Intra-particle CaO grains at each descrete radius from the particle center (i.e. subshell levels) react with sulfur species at an equal rate. The number of subshells used to describe particles is variable but should be at least 10 (Silcox, 1985).
- Individual grains shrink as CaO is consumed and swell as $CaSO_4$ is formed.
- Bulk diffusion to the sorbent particle surface is not limiting.
- Intra-particle diffusion is important. The effective diffusivity includes Knudsen and bulk-gas diffusion.
- Variable void-space due to grain swelling is calculated at each time step.
- Diffusion through $CaSO_4$ product layer is an important but not always a limiting resistance.
- Reaction of CaO with SO_2 is irreversible.
- The reaction order with respect to SO_2 can be half- or first-order.
- The reaction order with respect to oxygen for SO_2 capture is zero (i.e. oxygen is always in excess of SO_2).

One significant assumption that is made in the current sorbent-reaction submodel is that particles are instantaneously calcined as they enter with the coal particles in the primary inlet stream. Silcox (1985) showed that this is a reasonable assumption for sorbents injected into high-temperature regions. His calculations showed that particle heat-up and calcination occur over a short period of time relative to the time required for sulfination by SO_2. Silcox also notes that thermodynamic considerations rule out simultaneous calcination and sulfation if the sorbent is injected into the burner zone. If the sorbent is injected downstream of the burner zone in cooler flame regions, then simultaneous calcination and sulfation can occur. A model to predict joint calcination and sulfation was developed by Milne (1990) at the University of Utah. Whether or not this theory can be used to include simultaneous calcination in the current sorbent-reaction submodel framework has not been determined. The major limitation is the added complexity of the mathematical formulation and difficulty in obtaining numerical solutions.

Currently, a H_2S sulfation subroutine needs to be developed. This will require an examination of the controlling resistances in the particle and correlation of intrinsic reaction rates. There is a general lack of information in the open literature to elucidate the H_2S capture rates and important physical processes. Experimental data are currently being sought to complete this objective.

Model Prediction - A list of the Fortran subroutines for the SO_x/sorbent submodel is given in Table II.G-2. A description of input data is given in Table II.G-3. A hypothetical case has been predicted to demonstrate the model for combustion of subbituminous coal for which sulfur pollutant data are available (Asay, 1982). In the experiments, no sorbents were actually injected into the reactor. Figure II.G-4a shows the predicted particle trajectories for sorbents injected with the coal feed for the subbituminous combustion case and Figure II.G-4b show the changes in SO_2 concentration predicted after sorbent capture at two aft locations.

Table II.G-2. List of SO_x/Sorbent-Reaction Submodel FORTRAN Subroutines

Subroutine	Description
calcsj	Calculates sorbent particle number density
calso2	Solves finite difference equation for SO_2 species continuity
calh2s	Solves finite difference equation for H_2S species continuity
sorb0	Reads in input data from *filename*.dat and initializes sorbent particle number density
sorpar	Main submodel driver, calculates source terms for SO_2 and H_2S (sulfur entering with the coal or gas inlet streams), determines if convergence is obtained, prints out final results
spsict	Performs particle trajectory integration and calculates the capture of SO_2 and H2S in each computational cell, also calculates sink terms for SO_2 and H_2S species continuity
sulfat	calculates the change in conversion of calcined $CaCO_3$ particles to $CaSO_4$ according to the shrinking-core model of Silcox (1985)
RATESX.INC	include statements unique to SO_x/sorbent-reactions submodel
SOXRTE.INC	

Table III.G-3. SO_X/Sorbent-Reactions Submodel Data Input Description

Input in PCGC-2 *filename*.dat

```
**************************** PCSORB ******************************
*************** SOX/H2S-SORBENT REACTIONS SUBMODEL  *************
   ****************************      ******************************
   3,1                                !NSLS,NPSS
   0.0200, 1340.                      !SPLOAD,SPDEN
   0.0000,0.0000,0.0000,              !YPS(ISL),ISL = 1,5
   20.00E-06,                         !PDS(IPS),IPS = 1,3
   1.0000,                            !PMFS(IPS),IPS = 1,5
   F  F                               !LSPBUG,LYPS
   0.9500,0.0200,                     !YPSH,YPSL
   0.3500,                            !PRKS(IPS),IPS = 1,5
```

Definition of Input data

Variable	Description
NSLS	number of starting location for sorbent particles
NPSS	number of particle sizes for sorbent particles
SPLOAD	sorbent particle loading (ratio of sorbent particle mass to the mass of gas in the primary inlet) (kg s-1)
SPDEN	sorbent particle density (*i.e.*, density of CaO) (kg m-3)
YPS(ISL)	particle starting location for isl particle trajectory
PDS(IPS)	particle diameter for ips particle size
PMFS(IPS)	particle mass fraction (fraction of sorbent mass) for ips particle size
LSPBUG	logical to specify intermediate debugging printout
LYPS	
YPSH	
YPSL	
PRK(IPS)	turbulent Prandtl-Schmidt number for sorbent particles
nsubsh	number of sorbent particle subsheil (specified in PARAMETER.INC)
nsnode	number of sorbent particle nodes (specified in PARAMETER.INC)
iorder	order of sorbent particle reaction with respect to SO2 (assigned in *sulfat.F*) iorder = 1; first order reaction iorder = 2; half order reaction

Work is in progress to verify that these first results are correct. Subsequently, the SO_x/sorbent reaction submodel will be evaluated for other cases. The data collected under Subtask 2.H (Huber, 1989) will be used to evaluate fuel-rich capture after a subroutine to predict H2S capture is added to the submodel.

Plans

During the upcoming quarter, the evaluation of the SO2-capture submodel will continue. Completion of the H2S capture subroutine will be pursued. Researchers at The University of Utah (Silcox, 1990) may have experimental data available to develop H2S/sorbent-reaction rate expressions and diffusion expressions.